

Intelligent Weather Aware Scheme for Satellite Systems

Kamal Harb^{1,2}, Changcheng Huang¹, Anand Srinivasan², and Brian Cheng²

1 – Carleton University, 1125 Colonel By Drive, Ottawa, Ontario, Canada K1S 5B6

2 – EION Wireless, 945 Wellington Street, Ottawa, Ontario, Canada K1Y 2X5

Email: kharb@sce.carleton.ca

Abstract— Rain, snow, gaseous, cloud, fog, scintillation and other atmospheric properties can have a distorting effect on signal fidelity of Ku and Ka bands, thus resulting in excessive digital transmission error. This loss of signal is commonly referred to as signal attenuation. Signal attenuation impacts the QoS in wireless and satellite networks. Accurately predicting channel attenuation due to atmospheric conditions can enable mitigation planning by adaptively selecting appropriate modulation, coding, transmitted power level, transmission rate and configured frame size. The aim of this paper is to estimate different attenuations using predicted signal-weather correlated database in collaboration with ITU-R propagation models combined with interpolation methods, gateway, and ground terminal characteristics. A three dimensional relationship is proposed among these attenuations with respect to propagation angle and rainfall rate [1]-[8]. The outcome is key factor in diagnosing, adjusting and improving satellite signal power, modulation and coding schemes, monitored and controlled altogether by a powerful and efficient intelligent-based attenuation countermeasure system. These results will lead to an enhanced back propagation-learning algorithm that is used to iteratively tune the IS with returned SNR values to activate the weighted Modulation/Codepoint to its optimal values, depending on actual or predicted weather conditions, configuration settings and tolerance/safety margins for SLA commitment.

Index Terms— Intelligent System (IS), International Telecommunications Union - Radiocommunications (ITU-R), Quality of Service (QoS), Rain Attenuation (RA), Service Level Agreements (SLA), and Signal to Noise Ratio (SNR).

I. INTRODUCTION

Propagation impairments including rain, gaseous absorption, cloud, fog and tropospheric scintillation attenuations affect satellite links at Ku and Ka bands. These impairments become particularly severe at frequencies above 10 GHz, especially for small aperture antenna such as Very Small Aperture Terminal and Television Receive Only [7] and [9]. Rain attenuation (RA) is considered a dominant impairment for satellite signals.

A number of prediction models are available for estimating individual components. However, methodologies that attempt to combine them in a cohesive manner are not widely available yet [10]. Furthermore, it is extremely hard to optimally manage satellite-available network resources that are impacted by attenuations, with link traffic engineering only - “Goldilocks Link Budgeting”. It is then absolutely necessary to correctly identify and predict the overall impact of every significant attenuation factors on QoS, be it location, transmission or propagation characteristics along any given path between satellite and ground terminals [11]-[13].

In the absence of detailed knowledge of occurrence

probabilities for different impairments, empirical approaches are taken by estimating their combined effects. Once the amounts of expected impairments are established, appropriate methods for mitigating impairments must be invoked. Some of these include adaptive coding, antenna beam shaping, site diversity, and up-link power control. Note that, Up-link power control is one of the most cost-effective attenuation mitigation techniques. It enhances link availability and performance.

In view of these analytical approaches, dealing with weather-impacted QoS and reliable satellite communications are currently non-existent. Other thrusts in satellite service providers are shifting their resolution towards intelligent-based prediction methods. These types of methods accurately predict relevant atmospheric metrics; by adaptively applying the prediction methods to regulate transmit power, transmission rate, modulation schemes and channel coding. Consequently, these methods will promptly adjust to new signal changes through the inter-connected network entities, before attenuation problems actually manifest themselves, to maintain end-to-end QoS requirements [11]-[16].

In this paper, we use ITU-R models to accurately compute rain, gaseous absorption, cloud, fog and tropospheric scintillation attenuations as a function of both propagation angle and rainfall rate. This data will supply the intelligent system (IS) with a mechanism to better estimate satellite networking parameters such as link and queuing characteristics. The derived parameters would enable the IS to maintain QoS and SLAs.

The remaining sections of this paper are organized as follows: In section II, we calculate rainfall rate; section III, computes rain, gaseous, cloud, fog, and scintillation attenuations. It is then followed by a simulation and analysis of atmospheric attenuation. In section IV, SNR estimation and intelligent weather aware scheme for satellite system are presented. Finally, conclusions are outlined in section V.

II. RAINFALL RATE CALCULATION

Data files collected from ITU-R for P_R , M_C and M_S represent a weather characteristic model to derive rainfall rate at different X (Longitude degree) and Y (Latitude degree) locations. These data files contain numerical values for the variables: $P_R(X, Y)$, $M_C(X, Y)$ and $M_S(X, Y)$ respectively. Data files *Lat* and *Long* contain latitude and longitude for each data entry in all files [1]-[4], [6] and [8].

In the case presented, Rainfall rate is a function of probability used to determine atmospheric attenuations. It seems to correlate very closely with the volume of raindrops along the

path of propagation. Thus, rainfall rate can be computed by:

1)- Extracting variables P_R , M_C and M_S for the four points closest in *Lat* and *Long* to the geographical coordinates (X and Y) of the desired location. Latitude grid ranges $\{90^\circ \text{ N to } -90^\circ \text{ S}\}$, and longitude grid ranges $\{0 \text{ to } 360^\circ\}$ both for 1.5° steps. If the location falls on the grid, we will take these values as is from the given ITU-R tabulated data. Otherwise, we perform a Bi-Linear interpolation to the four closest grids.

2)- Deriving percentage probability of rainfall in an average year, P_0 , based on calculated data collected from previous steps, where:

$$P_0(X, Y) = P_R(X, Y) \left(1 - e^{-0.0117 (M_S(X, Y) / P_R(X, Y))} \right) \quad (1)$$

a. If $P_R = 0$, the result of this operation will be undetermined and consequently rainfall intensity will also be zero. In this case we shall stop the procedure.

b. If $P_R \neq 0$, we shall derive rainfall rate from exceeded percentage probability of interest p , where p should be $\leq P_0$, otherwise $P_0 = 0$ and the following steps will not be required:

$$a = 1.11, \quad b = \frac{(M_c(X, Y) + M_s(X, Y))}{22932 P_0} \quad \text{and} \quad c = 31.5 * b \quad (2)$$

$$A = a * b, \quad B = a + c * \ln(p / P_0(X, Y)) \quad \text{and} \quad C = \ln(p / P_0(X, Y)) \quad (3)$$

then, rainfall rate will be:

$$R_p(X, Y) = \frac{-B + \sqrt{B^2 - 4 * A * C}}{2 * A} \quad \text{mm/hr} \quad (4)$$

For example, rainfall rate value $R_p = 4.1957 \text{ mm/hr}$ at Hazelton station, for longitude $X = 114.4166 \text{ W}$, latitude $Y = 62.4182 \text{ N}$, and $p = 0.01\%$. If $P_0 = 0 \Rightarrow R_p$ from (4) will also be zero.

III. DIFFERENT ATTENUATIONS CALCULATION

III. 1 Rain Attenuation

Long-term statistics of slant-path RA for any given location at frequencies up to 55 GHz is provided using ITU-R estimates. Fig. 1 shows the relationship of signal propagation parameters. Other required parameters are: Frequency $f \text{ (GHz)}$, latitude of earth station $\rho_e \text{ (degree)}$ and effective radius of Earth $R_e \text{ (km)}$. With respect to altitude where rain extends during periods of precipitation, we can compute RA's behaviour based on frequency sample (F_i), for any location and applicable frequency, the following procedure has been recommended:

1)- If no specific information is available: the mean 0° C isotherm height - with resolution of 1.5° in both latitude and longitude - above mean sea level h_0 could be obtained from ITU-R data file *HEIGHT0.txt* [6].

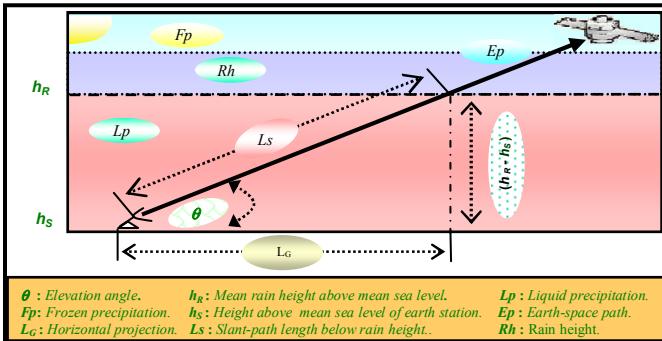


Fig. 1. Earth-Space Path

2)- Mean rain height above mean sea level, h_R , can be obtained from 0° C isotherm h_0 as: $h_R = h_0 + 0.36 \text{ km}$. (5)

3)- Slant-path length, L_S , can be computed as follows:

$$\text{i- } \theta < 5^\circ: L_S = \frac{2(h_R - h_S)}{\left(\sin^2 \theta + \frac{2(h_R - h_S)}{R_e} \right)^{1/2} + \sin \theta} \quad \text{km} \quad (6a)$$

$$\text{ii- } \theta \geq 5^\circ: L_S = \frac{(h_R - h_S)}{\sin \theta} \quad \text{km} \quad (6b)$$

if $(h_R - h_S) \leq 0 \Rightarrow$ predicted RA for any time percentage is equal to zero and the following steps are not required.

4)- Calculate horizontal projection, L_G , of slant-path length from: $L_G = L_S \cos \theta \text{ km}$ (7)

5)- Find rainfall rate, R_p , for exceeded $p = 0.01\%$ of an average year. If $R_{0.01} = 0 \Rightarrow RA = 0$ for any time percentage and the following steps are not required.

6)- Compute specific attenuation, γ_p , using frequency-dependent coefficients as given in [3] for k , α and rainfall rate, R_p , calculated earlier for $p = 0.01\%$, by using:

$$\gamma_{0.01} = K (R_{0.01})^\alpha \quad \text{dB/km} \quad (8)$$

For linear and circular polarization and for all path geometries, coefficients in (8) can be computed from (9) and (10) as:

$$K = \left[K_H + K_V + (K_H - K_V) \cos^2 \theta \cos 2\tau \right] / 2 \quad (9)$$

$$\alpha = \left[K_H \alpha_H + K_V \alpha_V + (K_H \alpha_H - K_V \alpha_V) \cos^2 \theta \cos 2\tau \right] / 2k \quad (10)$$

where K_V , α_V and K_H , α_H are constant coefficients of vertical and horizontal polarizations respectively. Also, θ is the path propagation angle and τ is the polarization tilt angle relative to the horizontal, equal to 45 degree for circular polarization.

7)- Calculate horizontal reduction factor, r_p , for $p = 0.01\%$:

$$r_{0.01} = \frac{1}{1 + 0.78 \sqrt{\frac{L_G \cdot \gamma_{0.01}}{f}} - 0.38 (1 - e^{-2L_G})} \quad (11)$$

8)- Calculate vertical adjustment factor, v_p , for $p = 0.01\%$:

$$\sigma = \tan^{-1} \left(\frac{h_R - h_S}{L_G \cdot r_{0.01}} \right) \quad \text{degrees} \quad (12)$$

For $\sigma > \theta$, the actual slant-path length L_R will be:

$$L_R = \frac{L_G \cdot r_{0.01}}{\cos \theta}, \quad \text{else } L_R = \frac{(h_R - h_S)}{\sin \theta} \quad \text{km} \quad (13)$$

$$\text{if } |\rho_e| < 36^\circ \Rightarrow \chi = 36 - |\rho_e|, \quad \text{else } \chi = 0 \quad \text{degree} \quad (14)$$

$$v_{0.01} = \frac{1}{1 + \sqrt{\sin \theta} \left(31 \left(1 - e^{-\left(\frac{\theta}{1+\chi} \right)} \right) \sqrt{\frac{L_R \cdot \gamma_{0.01}}{f^2}} - 0.45 \right)} \quad (15)$$

9)- Effective path length is: $L_E = L_R \cdot v_{0.01} \text{ km}$ (16)

10)- Predicted exceeded RA for $p = 0.01\%$ of an average year is obtained from: $A_{0.01} = \gamma_{0.01} \cdot L_E \text{ dB}$ (17)

11)- For other exceeding percentages of an average year ranging from 0.001% to 5% , estimations of RA can be computed from (17) for an average year as follows:

$$\text{if } p \geq 1\% \quad \text{or} \quad |\rho_e| \geq 36^\circ \Rightarrow \beta = 0,$$

else if $p < 1\%$ or $|\rho_e| < 36^\circ$ and $\theta \geq 25^\circ \Rightarrow \beta = -0.005 (|\rho_e| - 36)$, otherwise $\beta = -0.005 (|\rho_e| - 36) + 1.8 - 4.25 \sin \theta$ (18)

$$A_{rain}(p) = A_{0.01} \left(\frac{p}{0.01} \right)^{-0.655 + 0.033 \ln(p) - 0.045 \ln(A_{0.01}) - \beta(1-p) \sin \theta} \quad dB \quad (19)$$

Note: the above RA equation was tested by ITU-R and found to have the most accurate overall results of all tested models.

We propose to compute RA as a function of any frequency (f) value as: $A_{rain}(f_n) = \gamma_R(f_n) \cdot L_E(f_n) dB$ (20)

Also, for any specific frequency ranging from 7 to 55 GHz can be obtained from:

$$H(\varphi(f_{n-1}), \varphi(f_n), A_{rain}(f_{n-1})) = 1.12 \times 10^{-3} \dots \left(\frac{\varphi(f_n)}{\varphi(f_{n-1})} \right)^{0.5} (\varphi(f_{n-1}) A_{rain}(f_{n-1}))^{0.55} \quad (21)$$

$$A_{rain}(f_n) = A_{rain}(f_{n-1}) \left(\frac{\varphi(f_n)}{\varphi(f_{n-1})} \right)^{(1-H(\varphi(f_{n-1}), \varphi(f_n), A_{rain}(f_{n-1})))} \quad dB \quad (22)$$

where $A_{rain}(f_{n-1})$ and $A_{rain}(f_n)$ are the equiprobable values of excess RA at frequencies (f_{n-1}) and (f_n), respectively [1].

Methods explained so far, are used to investigate the dependence of RA statistics on propagation angle, rainfall rate, polarization, probability and frequency. Thus, if reliable attenuation data measured at any specific frequency is available, the adjusted empirical formulas shown in (20)-(22) will then provide RA as a function of its preceding frequency. That is, once we have RA at any lower frequency, we can then compute RA of upper level based on the obtained one and so on until we reach the maximum desired frequency [1] and [4].

Moreover, this method provides high CPU efficiency since we do not have to repeat the entire calculation from (8) for each frequency, as is the case of existing solutions [8]. Also, this paper introduces RA in (23) as a function of rainfall rate (R_p) and propagation angle (θ) by combining several equations:

$$A_{rain}(\theta, R_p) = \gamma_R(\theta, R_p) \cdot L_E(\theta, R_p) \quad dB \quad (23)$$

where $A_{rain}(\theta, R_p)$ represents RA for a wide range of rainfall rate and propagation angle as shown in Fig. 2.

This method provides a useful general tool for scaling RA according to these parameters. Also, this model helps to provide designers with a perceptible view of approximate RA values that can be computed at any desired location (X and Y), for a different propagation angle, for any rainfall rate, and for any specific uplink or downlink frequencies.

III.2 Gaseous Attenuation

In this section, analytical solution is presented to calculate attenuation due to atmospheric gases. Thus, predicting gaseous attenuation requires an accurate model that allows us to represent the specific attenuation mathematically. It can be calculated by summing the effects of all the significant resonance lines given in ITU-R P.676 as:

1. Specific Attenuation:

A- For dry air, the attenuation γ_o (dB/km) is given by the following equation for the frequency of interest ($f \leq 54$ GHz):

$$\gamma_o = \left[\frac{7.2 r_t^{2.8}}{f^2 + 0.34 r_{ph}^2 r_t^{1.6}} + \frac{0.62 \xi_3}{(54 - f)^{1.16} \xi_1 + 0.83 \xi_2} \right] f^2 r_{ph}^2 \times 10^{-3} \quad (24)$$

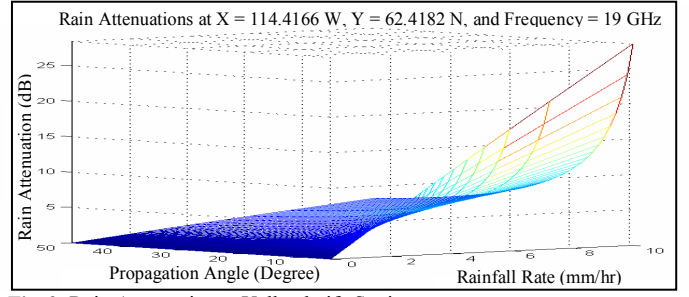


Fig. 2. Rain Attenuation at Yellowknife Station

$$\text{with: } \xi_1 = \varphi(r_{ph}, r_t, 0.0717, -1.8132, 0.0156, -1.6515) \quad (25a)$$

$$\xi_2 = \varphi(r_{ph}, r_t, 0.5146, -4.6368, -0.1921, -5.7416) \quad (25b)$$

$$\xi_3 = \varphi(r_{ph}, r_t, 0.3414, -6.5851, 0.2130, -8.5854) \quad (25c)$$

$$\varphi(r_{ph}, r_t, a, b, c, d) = r_{ph}^a r_t^b \exp[c(1 - r_{ph}) + d(1 - r_t)] \quad (26)$$

B- For water vapour, the attenuation γ_w (dB/km) is given by:

$$\gamma_w = \left\{ \frac{3.98\eta_1 \exp[2.23(1-r_t)]}{(f-22.235)^2 + 9.42\eta_1^2} g(f, 22) + \frac{11.96\eta_1 \exp[0.7(1-r_t)]}{(f-183.31)^2 + 11.14\eta_1^2} \right. \\ + \frac{0.081\eta_1 \exp[6.44(1-r_t)]}{(f-321.226)^2 + 6.29\eta_1^2} + \frac{3.66\eta_1 \exp[1.6(1-r_t)]}{(f-325.153)^2 + 9.22\eta_1^2} \\ + \frac{25.37\eta_1 \exp[1.09(1-r_t)]}{(f-380)^2} + \frac{17.4\eta_1 \exp[1.46(1-r_t)]}{(f-448)^2} \\ + \frac{844.6\eta_1 \exp[0.17(1-r_t)]}{(f-557)^2} g(f, 557) + \frac{290\eta_1 \exp[0.41(1-r_t)]}{(f-752)^2} g(f, 752) \\ \left. + \frac{8.3328 \times 10^4 \eta_2 \exp[0.99(1-r_t)]}{(f-1780)^2} g(f, 1780) \right\} f^2 r_t^{2.5} \rho \times 10^{-4} \quad (27)$$

$$\text{with } \eta_1 = 0.955 r_{ph} r_t^{0.68} + 0.006 \rho, \eta_2 = 0.735 r_{ph} r_t^{0.5} + 0.0353 r_t^4 \rho \quad (28)$$

$$\text{and } g(f, f_i) = 1 + \left(\frac{f - f_i}{f + f_i} \right)^2 \quad (29)$$

where ph : pressure (hPa), $r_{ph} = ph/1013$, $r_t = 288/(273 + t)$, ρ : water-vapour density (g/m^3), f : frequency (GHz), and t : mean temperature values ($^\circ C$), can be obtained from ITU-R P.1510 when no adequate temperature data is available.

2. Slant Path Equivalent Height:

The slant path attenuation depends on the distribution along the path of meteorological parameters such as temperature (t), pressure (ph) and humidity (ρ). Thus, it varies with location (X, Y), month of the year, height of a station above sea level (h_s) and the propagation angle (θ).

A- For dry air, the equivalent height is given by:

$$h_o = \frac{6.1}{1 + 0.17 r_{ph}^{-1.1}} (1 + t_1 + t_2 + t_3) \quad (30)$$

$$\text{where } t_1 = \frac{4.64}{1 + 0.066 r_{ph}^{-2.3}} \exp \left[- \left(\frac{f - 59.7}{2.87 + 12.4 \exp(-7.9 r_{ph})} \right)^2 \right], \quad (31a)$$

$$t_2 = \frac{0.14 \exp(2.12 r_{ph})}{(f - 118.75)^2 + 0.031 \exp(2.2 r_{ph})}, \quad (31b)$$

$$\text{and } t_3 = \frac{0.0114}{1 + 0.14 r_{ph}^{-2.6}} f \frac{-0.0247 + 10^{-4} f + 1.61 \times 10^{-6} f^2}{1 - 0.0169 f + 4.1 \times 10^{-5} f^2 + 3.2 \times 10^{-7} f^3} \quad (31c)$$

with the constraint that: $h_o \leq 10.7 r_{ph}^{0.3}$ when $f < 70$ GHz.

B- for water vapour, the equivalent height for $f \leq 350$ GHz is:

$$h_w = 1.66 \left(1 + \frac{1.39\sigma_w}{(f-22235)^2 + 2.56\sigma_w} + \frac{3.37\sigma_w}{(f-18331)^2 + 4.69\sigma_w} + \frac{1.58\sigma_w}{(f-3251)^2 + 2.89\sigma_w} \right) \quad (32)$$

Notice that water vapour has resonance at (22.235), (183.31) and (325.1) GHz respectively and that attenuation changes with the amount of water vapour in the atmosphere.

3. Path Attenuation for Earth-Space propagation angle between 5 and 70 degrees:

The above method calculates slant path attenuation of water vapour that relies on the knowledge of the profile of water-vapour pressure (or density) along the attenuation path. It provides useful general tool for scaling Gas according to these parameters. Thus, the approximate Gaseous values can be computed at any desired location (X and Y), for all ranges of angle and rainfall rate for a given uplink or downlink frequencies as shown in Fig. 3.

This paper proposes to obtain the path attenuation based on surface meteorological data using the cosecant law for a given propagation angle and rainfall rate, by combining several equations as:

$$A_{Gas}(\theta, R_p) = \frac{A_o + A_w}{\sin \theta} \quad dB \quad (33)$$

$$\text{where } A_o = h_o \gamma_o \text{ and } A_w = h_w \gamma_w \quad (34)$$

III.3 Clouds and Fog Attenuations

Clouds and fog can be described as a collection of smaller rain droplets or alternatively, as different interactions from rain as the water droplet size in fog and cloud is smaller than the wavelength of 3–30 GHz. These attenuations can be expressed in terms of rainfall rate and propagation angle for a specific frequency and temperature values, as shown in Fig. 4:

$$D_{p1} = ((\epsilon_0 - \epsilon_1) / (1 + (f/f_p)^2)) + ((\epsilon_1 - \epsilon_2) / (1 + (f/f_s)^2)) + \epsilon_2 \quad (35a)$$

$$D_{p2} = (f \cdot (\epsilon_0 - \epsilon_1) / (f_p \cdot (1 + (f/f_p)^2))) + (f \cdot (\epsilon_1 - \epsilon_2) / (f_s \cdot (1 + (f/f_s)^2))) \quad (35b)$$

$$\eta = (2 + D_{p1}) / D_{p2} \quad (36)$$

$$K_t = (0.819 * f) / (D_{p2} \cdot (1 + \eta^2)) \quad (37)$$

$$t_l = 300 / t_k, \text{ where } t_k = \text{Temperature (Kelvin)} \quad (38)$$

$$\epsilon_2 = 3.51, \epsilon_1 = 5.48, \text{ and } \epsilon_0 = 77.6 + 103.3(t_l - 1) \quad (39)$$

$$f_s = 590 - 1500(t_l - 1), \text{ and } f_p = 20.09 - 142(t_l - 1) + 294(t_l - 1)^2 \quad (40)$$

To obtain the predicted attenuation due to clouds for a given probability value, the statistics of the total columnar content of liquid water L_w (kg/m^2), which is an integration of liquid water density, M (kg/m^3), along a cross section of $1 m^2$ from surface to top of clouds for a given site, must be known yielding as shown in Fig. 4 for propagation angle ranging between

$$90^\circ \cdot \theta \cdot 5^\circ \text{ as: } A_{Cloud \ \& \ Fog}(\theta, R_p) = \frac{L_w \cdot K_t}{\sin \theta} \quad dB \quad (41)$$

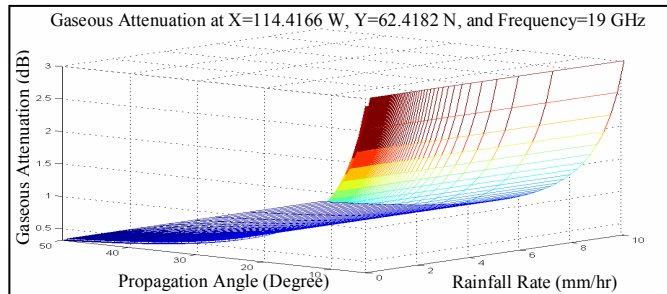


Fig. 3. Gaseous Attenuation at Yellowknife Station

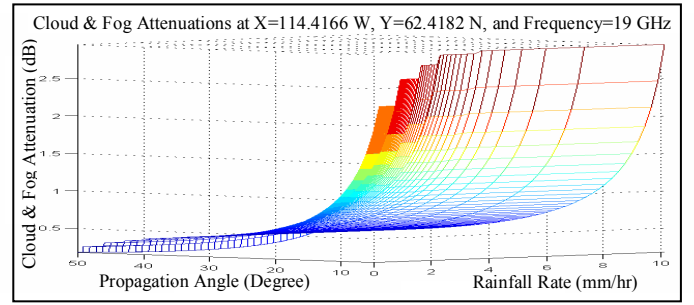


Fig. 4. Clouds and Fog Attenuations at Yellowknife Station

III.4 Scintillation Attenuation

The cumulative distribution of tropospheric scintillation is based on monthly or longer average surface of ambient temperature t ($^\circ C$). This distribution reflects the specific climate conditions of the site [17]. Following is a general technique for predicting it at different rainfall rate and propagation angle that is greater than 4° is shown in Fig. 5.

Calculate the standard deviation of the signal amplitude, σ_{ref} , used as reference: $\sigma_{ref} = 3.6 \cdot 10^{-3} + 10^{-4} \cdot N_{wet} \quad dB \quad (42)$

where N_{wet} : radio refractivity, given in ITU-R P.453. Calculate the effective path length L for $h_L = 1000$ m:

$$L = \frac{2 h_L}{\sqrt{\sin^2 \theta + 2 \cdot 35 \times 10^{-4} + \sin \theta}} \quad m \quad (43)$$

h_L : the height of the turbulent layer equal to 1000 m.

Estimate the effective antenna diameter, D_{eff} , from the geometrical diameter (m) of the earth-station antenna, D , and the antenna efficiency η : if unknown, $\eta = 0.5$ is used as:

$$D_{eff} = \sqrt{\eta} \cdot D \quad m \quad (44)$$

Calculate the antenna-averaging factor from:

$$g(x) = \sqrt{3.86(x^2 + 1)^{1/2} \cdot \sin \left[\frac{11}{6} \arctan \frac{1}{x} \right] - 7.08 x^{5/6}} \quad (45)$$

$$\text{with } x = 1.22 \cdot D_{eff} \cdot (f/L) \quad (46)$$

$$\sigma = \sigma_{ref} \cdot f^{7/12} \cdot \frac{g(x)}{(\sin \theta)^{1.2}} \quad (47)$$

Calculate time percentage factor, $a(p)$, for the time percentage, p , of concern in the range $0.01 < p \leq 50$:

$$a(p) = -0.061 \cdot (\log p)^3 + 0.072 \cdot (\log p)^2 - 1.71 \cdot \log(p) + 3.0 \quad (48)$$

Calculate the scintillation fade depth as:

$$A_{Scintillation}(\theta, p) = a(p) \cdot \sigma(\theta) \quad dB \quad (49a)$$

It can also be written after mathematical manipulation as:

$$A_{Scintillation}(\theta, R_p) = a(p) \cdot \sigma(\theta) \quad dB \quad (49b)$$

The probability of attenuation (p) not exceeding ranges from 0.001% to 50% and the carrier frequency (f): $4 \leq f \leq 30$ GHz.

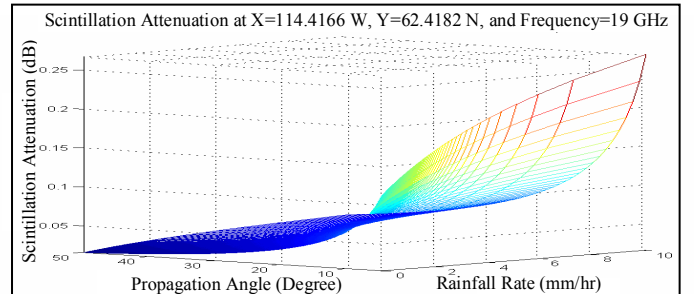


Fig. 5. Scintillation Attenuation at Yellowknife Station

III.5 Atmospheric Attenuation

In this section atmospheric attenuation is calculated based on rain, gas, cloud, fog and scintillation attenuations. These attenuations for systems operating at frequencies above 10 GHz [13] - especially those operating with low propagation angles and/or margins - must be considered along with the effect of multiple sources of simultaneous occurring.

The required input parameters for the above attenuations are:

$A_{Rain}(\theta, R_p)$: attenuation due to rain, as estimated in (23).

$A_{Gas}(\theta, R_p)$: gaseous attenuation due to water vapour and oxygen, as estimated in (33).

$A_{Cloud\&Fog}(\theta, R_p)$: cloud and fog attenuation, as by (41).

$A_{Scintillation}(\theta, R_p)$: attenuation due to tropospheric scintillation, as estimated in (49).

A general method for calculating these attenuations for a given propagation angle and Rainfall rate, $A_W(\theta, R_p)$, is given by:

$$A_W = A_{Gas} + \sqrt{(A_{Rain} + A_{Cloud\&Fog})^2 + A_{Scintillation}^2} \text{ dB} \quad (50)$$

where $A_{Cloud\&Fog}(\theta, R_p) \cong A_{Cloud\&Fog}(\theta, R_{1\%})$ for $p < 1.0\%$ (51a)

and $A_{Gas}(\theta, R_p) \cong A_{Gas}(\theta, R_{1\%})$ for $p < 1.0\%$ (51b)

Equations (51a) and (51b) take into consideration that a large part of cloud and gaseous attenuations are already included in RA prediction for time percentage below 1% [8].

This prediction method was tested using contour rain map in [3], and procedures set out in ITU-R P.311. The results were found to be in good agreement with the available measurement data for all latitudes for the probability ranging from 0.001% to 1% as shown in Fig. 6 with an overall r.m.s. error about 35%. Whereas, the overall r.m.s. error was found to be about 25% when using multi-year Earth-space data.

Therefore, due to the dominance of different effects at different probabilities as well as the inconsistent availability of test data at different probability levels, some variations of r.m.s. errors occur across the distribution of different probabilities. Thus, knowing this data will be an immense asset to support analysis for budgeting the operational satellite networking parameters around the world.

IV. SIGNAL TO NOISE RATIO (SNR) CALCULATION

By definition, SNR is a measure of signal strength for satellite signal relative to attenuations and background noise. Based on previous calculations for different attenuations, we are able to estimate SNR accurately. SNR is usually measured in decibels (dB) and is calculated as follows [16]:

Thermal noise power Spectral density is: $N_0 = K \cdot T$,

$K = 1.38 \cdot 10^{-23} \text{ Ws/K} = -228.6 \text{ dB Ws/K}$ and

T (effective noise temperature) = $T_a + T_r$,

T_a Noise temperature of the Antenna is represented in Table 1,

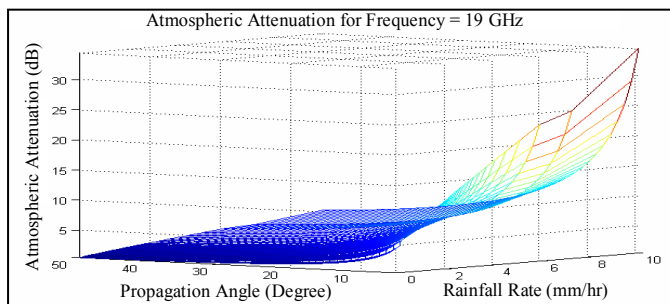


Fig. 6. Atmospheric Attenuation at Yellowknife Station

Table 1. Noise Temperature in Antenna

Antenna Noise Temperature T_a (Kelvin)		
Directional satellite antenna	Earth from space	290 K
Directional terminal antenna	Space from earth at 90° elev.	3 – 10 K
	Space from earth at 10° elev.	≈ 80 K
	Sun (1...10 GHz)	$10^5 \dots 10^4$ K
Hemispherical terminal antenna	At night	290 K
	Cloudy sky	360 K
	Clear sky with sunshine	400 K

and T_r (Noise temperature of the Receiver) = $(10^{N_r/10} - 1) \cdot 290$ (52) where noise figure of Low-noise amplifier, $N_r \approx 0.7 - 2 \text{ dB}$. Thus, ratio between signal and noise power spectral density is:

$$\frac{C}{N_0} = \frac{C}{K \cdot T} = \frac{P_r}{K \cdot T} \dots \quad (53a)$$

$$\dots = \frac{P_t \cdot G_t}{A_t} \cdot \frac{G_r}{K \cdot T} = \frac{EIRP}{A_t} \cdot \frac{G_r}{K \cdot T}$$

$$\left. \frac{C}{N_0} \right|_{dB} = P_t + G_t - A_t + G_r - K - T \quad (53b)$$

Where A_t (total attenuation) = $A_W + A_0$ (free space loss), such as $A_0 = (4 \cdot \pi \cdot d / \lambda)^2$, d = distance between transmitter and receiver, λ (wavelength) = c/f , P_t and P_r are transmitted and received power, and G_t and G_r are antenna gain at transmitter and receiver sides respectively. By considering a receive filter with noise of equivalent bandwidth (B_r), the noise power N will be: $N_0 \cdot B_r = K \cdot T \cdot B_r$, and

$$SNR = \frac{C}{N} = \frac{C}{N_0} \cdot \frac{1}{B_r} \quad (54)$$

IV.1 Signal to Noise Ratio Adjustment

Several factors such as power, modulation, etc., can perform an immense role in improving SNR and in maximizing system throughput and availability of the link. In this section, a new proposed IS is introduced, as shown in Fig. 7, to overcome different weather conditions. Thus, by controlling the above mentioned factors that supply the IS, a path is given to allow an efficient mechanism to better estimate satellite networking parameters such as link and queuing characteristics. These derived parameters would enable the IS to maintain SNR by adaptively adjusting signal power, transmission rate, coding, and modulation under unpredictable weather conditions.

By definition, E_s (symbol energy) = $C \cdot T_s = C / R_s$, where

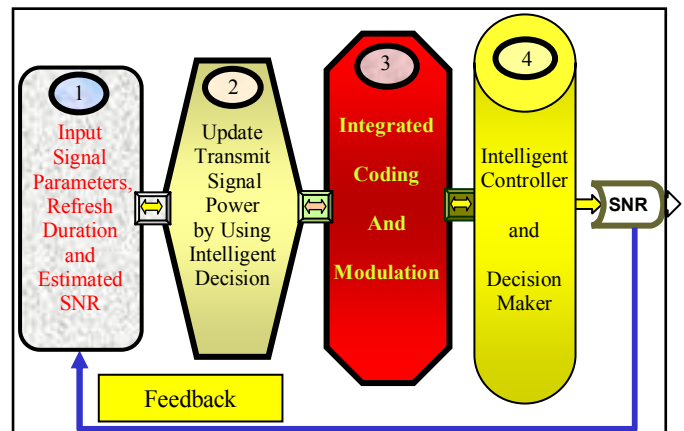


Fig. 7. Intelligent Weather Aware Scheme for Satellite Systems

transmission rate R_s (symbol/sec) is inversely equivalent to T_s (symbol duration) = $1/R_s$ and energy-to-noise power density per symbol is: $\frac{E_s}{N_0} = \frac{C}{N_0} \cdot T_s$, where:

$$\frac{E_s}{N_0} = \frac{C}{N_0} \cdot \frac{1}{R_s} \text{ or } \left. \frac{E_s}{N_0} \right|_{dB} = \frac{C}{N_0} - R_s \quad (55a)$$

$$\left. \frac{E_s}{N_0} \right|_{dB} = P_t + G_t - A_t + G_r - T - K - R_s \text{ dB} \quad (55b)$$

E_s / N_0 : Determines bit error rate for digital transmission scheme.

Fig. 7 illustrates a manner for changing parameters of the communication system in order to overcome the deteriorating effect of atmospheric impairments, and to increase reliability of the data transmitted throughout the channel. In the first stage, the system holds input signal parameters such as frame size, propagation angle, etc. and SNR estimated values that were compared against threshold level, in a single database. The result should be greater than or at least equal to this level.

In the second stage, based on SNR values, either the intelligent system will decide to increase transmit power for a maximum limit of -30 dB (0 dBm), or to skip to the next stage. Next, SNR value will be checked among Modulation and Coding values given in Table 2. If this value can be reached by using any of the mentioned table combinations, then the system will go to the final stage.

In the last stage, the system will compromise among different SNR achieved outputs and make decision based on the intelligent controller according to available parameters and requirements. The given feedback will keep looping until a satisfactory value is reached.

Thus, this system can also change data rate, frame size, frequency, etc. in order to adjust SNR, in cases such as unpredicted bad weather condition, by using Refresh Duration that is located in the first stage.

Fig. 8 and Fig. 9 compare the outputs of SNR ranges before and after adjustments respectively. Where SNR fell between (-40 ~ -14) dB, for power transmits from (-85 ~ -72) dB, and was transformed after intelligent improvements to fall within modulation and coding boundaries of allowable used database. The adjusted output SNR ranges from (-1.5 ~ 22) dB, (-48 ~ -35) dB for transmitted power, and (0 ~ 11) mm/hr for same rainfall rate in both results.

Note that, there is limits of increasing transmit power up to around -30 dB. Once this value has been reached, Mod/Cod selection should match in order to adjust SNR as per Table 2. Consequently, Fig. 7, Fig. 9 and Table 2 show throughput

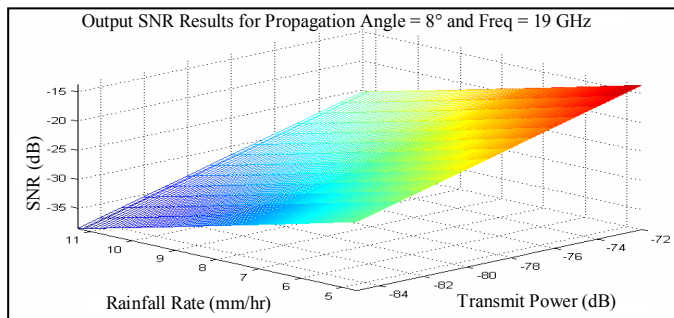


Fig. 8. Output SNR at Yellowknife Station

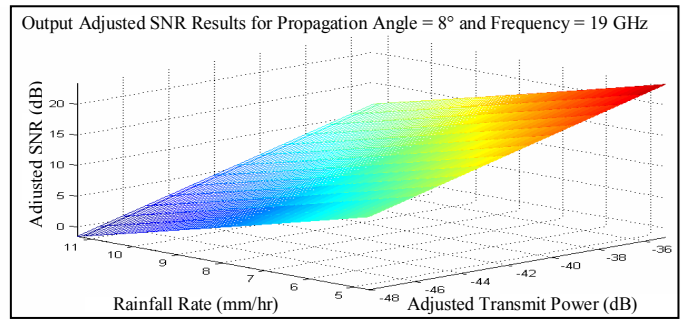


Fig. 9. Output adjusted SNR at Yellowknife Station

enhancements for wireless communication systems. They also create a robust IS by allowing designers to work with flexible ranges by applying various combinations of modulation, coding and transmit power for any unpredicted weather conditions.

Table 2. Forward Link Modes and Performance for $\theta = 8^\circ$ and $f = 19 \text{ GHz}$

Modulation	LDPC Code Identifier	E_s/N_0 [dB] Measured/ Estimated	Transmit Power [dB]	Rainfall Rate [mm/hr]
QPSK	1/4	-1.5/-1.31	-55	10.80
QPSK	1/3	-0.3/-0.23	-53	11.45
QPSK	2/5	0.7/0.74	-54	10.06
QPSK	1/2	1.3/1.49	-52	10.94
QPSK	3/5	3.2/3.41	-51	10.29
QPSK	2/3	3.8/4.0	-50	10.53
QPSK	3/4	4.8/5.06	-48	11.23
QPSK	4/5	5.3/5.41	-49	10.30
QPSK	5/6	5.8/5.91	-56	5.14
QPSK	8/9	6.8/6.83	-53	6.54
8PSK	3/5	6.4/6.43	-49	9.58
8PSK	2/3	7.3/7.32	-52	6.89
8PSK	3/4	8.6/8.64	-53	5.32
8PSK	5/6	10.0/10.17	-47	8.37
8PSK	8/9	11.4/11.75	-45	8.78
16PSK	2/3	9.6/9.61	-55	3.36
16PSK	3/4	10.9/11.09	-51	5.02
16PSK	4/5	11.8/11.82	-46	7.92
16PSK	5/6	12.4/12.45	-48	6.12
16PSK	8/9	13.7/13.71	-42	9.32

V. CONCLUSIONS

Signal attenuations caused by rain, gaseous, cloud, fog and scintillation attenuations limit satellite's QoS links and system availability that operate at frequencies above Ku-band.

The proposed method improves QoS by providing accurate estimates for different weather behaviours that lead us to adjust SNR output in lieu of a wide range of rainfall rate and transmit power, for any specific modulation, coding, propagation angle, frequency, transmission rate, and location. Also, it enhances back propagation-learning algorithm by computing attenuation periodically to iteratively tune the IS with returned SNR values and by activating the weighted Modulation/Codepoint optimal values, depending on actual or predicted weather conditions.

Hence, the proposed intelligent System gives designers the flexibility at any location to apply various combinations of modulation, coding, transmission power, frequency, propagation angle, and transmission rate in order to maximize satellite's system throughput and QoS for any unpredicted weather condition.

ACKNOWLEDGMENTS

The authors wish to thank:

- Kalai Kalaichelvan and Rama Munikoti of EION, Bharat Rudra of OCE, and Derek Best of Precarn for supporting this project
- Andre Bigras and Abdul Lakhani of Telesat for verifying the applicability and usefulness for satellite systems

REFERENCES

- [1] K. Harb, A. Srinivasan, C. Huang and B. Cheng, "Prediction method to Maintain QoS in Weather Impacted Wireless and Satellite Networks", Proc. of the IEEE, SMC Conference, Montreal, QC, Canada, pp. 4008 – 4013, Oct. 2007.
- [2] ITU-R, "Characteristics of precipitation for propagation modeling", Recommendation ITU-R P.837-4, 2001, P. Series Fascicle, Radio wave propagation, International Telecommunication Union, Geneva.
- [3] ITU-R, "Specific attenuation model for rain for use in prediction methods", Recommendation ITU-R P. 838-3, 2003, P. Series Fascicle, Radio wave propagation, International Telecommunication Union.
- [4] K. Harb, A. Srinivasan, C. Huang and B. Cheng, "QoS In Weather Impacted Satellite Networks", Proc. of the IEEE Pacific Rim Conference on Communications, Computers and Signal Processing, Victoria, B.C., Canada, pp. 178 – 181, Aug. 2007.
- [5] R. K. Crane, "Prediction of the Effects of Rain on Satellite Communication Systems", Proc. of the IEEE, Vol. 65, No.3, pp. 456-474, March 1977.
- [6] ITU-R, "Rain height model for prediction methods", Recommendation ITU-R P.839-3, 2001, P. Series Fascicle, Radio wave propagation, International Telecommunication Union, Geneva.
- [7] A. Dissanayake, J. Allnut, F. Haidara, "A prediction model that combines rain attenuation and other propagation impairments along Earth-satellite paths", IEEE Trans. on Antennas & Propagation, Volume 45, Issue 10, pp. 1546 – 1558, Oct. 1997.
- [8] ITU-R, "Propagation data and prediction method required for the design of Earth-space Telecommunication systems", Recommendation ITU-R P.618-7, 2001, P. Series Fascicle, Radio wave propagation, International Telecommunication Union, Geneva.
- [9] T. Boonchuk, N. Hemmakorn, P. Supnithi, M. Iida, K. Tanaka, K. Igarashi, Y. Moriya, " Rain Attenuation of Satellite link in Ku-band at Bangkok ", Information, Communications and Signal Processing, Fifth International Conference, pp. 1093 – 1096, Dec. 2005.
- [10] Garcia-Lopez, J.A. et al, (1988), " Simple Rain Attenuation Prediction Method for Satellite Radio Links," IEEE Trans. on Antennas & Propagation, Vol. 36, No. 3, March 1988.
- [11] Karasawa, Y.T., & T. Matsudo, " Characteristics of fading on low-elevation angle Earth-space paths with concurrent rain attenuation and scintillation, " IEEE Trans. on Antennas & Propagation, Vol. 39, No. 5, pp. 657 – 661, May 1991.
- [12] A. Safaai-Jazi, H. Ajaz, W. L. Stutzman, " Empirical models for rain fade time on Ku- and Ka-band satellite links ", IEEE Trans. on Antennas & Propagation, Vol. 43, No. 12, pp. 1411 – 1415, Dec. 1995.
- [13] W. J. Vogel, J. Goldhirsh, " Multipath fading at L band for low elevation angle, land mobile satellite scenarios ", IEEE selected areas in communications, Vol. 13, No. 2, pp. 197 – 204, Feb. 1995.
- [14] A. A. Aboudebra, K. Tanaka, T. Wakabayashi, S. Yamamoto, H. Wakana, " Signal fading in land-mobile satellite communication systems: statistical characteristics of data measured in Japan using ETS-VI ", IEEE Trans. on Microwave, Antennas & Propagation, Vol. 146, No. 5, pp. 349 – 354, Oct. 1999.
- [15] Ippolito, Louis J., & Thomas A. Russell (1993), "Propagation Considerations for Emerging Satellite Communications Applications," Proc. of the IEEE, Vol. 81, No. 6, pp. 923-929, June 1993.
- [16] E. Lutz, M. Werner, A. Jahn, *Satellite Systems for Personal and Broadband Communications*, pages 47-82. Springer, New York, 2000.
- [17] K. Yasukawa, M. Yamada, Y. Karasawa, " Tropospheric scintillation in the 14/11-GHz bands on Earth-space paths with low elevation angles ", IEEE Trans. on Antennas & Propagation, Vol. 36, No. 4, pp. 563 - 569, April 1988.